Landslides (2020) 17:1269–1281
DOI 10.1007/s10346-020-01357-y
Received: 4 August 2019
Accepted: 21 January 2020
Published online: 13 February 2020


Yang Ren · Tianbin Li · Simeng Dong · Jieling Tang · Demin Xue

# Rainfall-induced reactivation mechanism of a landslide with multiple-soft layers

**Abstract** A study on the site investigation data from the Chengnan landslide, which was a partially reactivated ancient landslide in Meigu County, Xichang City, China, is presented. To explore the reactivation mechanism of the Chengnan landslide, we conducted site investigation, surface displacement monitoring, deep displacement monitoring, finite element analysis, and limit the equilibrium analysis of the Chengnan landslide. The results indicated that the Chengnan landslide experienced multiple reactivations. It was initially reactivated in 2002 along the first clay layer at a depth of 14 m; after comprehensive treatment measures, which included excavating to reduce loads, improving the drainage system, and installing anti-sliding piles in 2006, further deformation was prevented. However, heavy rainfall in 2007 caused groundwater infiltration, softening the second clay layer at a depth of 28 m and transforming it into a new sliding surface (i.e., the second sliding surface). Consequently, Chengnan landslide was reactivated again along the second sliding surface, and the anti-sliding piles moved together with upper sliding body along the second sliding surface because this sliding surface was located deeper than the anti-sliding piles. Based on the results of this study, a multilayer creeping–tension mechanism controlled by multiple soft layers of the Chengnan landslide was proposed. This interesting case study should be considered from a scientific and technical point of view; some valuable suggestions for site investigation and treatment of this kind of landslide are also proposed.

**Keywords** Landslide · Rainfall · Soft layers · Displacement monitoring · Finite element analysis · Reactivation mechanism

## Introduction

Landslides are a common natural hazard. Ancient landslides can be defined as landslides that occurred thousands of years ago and became stable for a considerable time afterward. However, an ancient landslide can be reactivated entirely or partially by several factors, including heavy rainfall, road excavation, and earthquakes. Numerous researchers have studied the reactivation of ancient landslides. Some scholars studied ancient landslides reactivated by road excavation (Anbarasu et al. 2010; Ferrari et al. 2011; Massey et al. 2013; Wang et al. 2014; Xue et al. 2014). Heavy seasonal rainfall has also been considered as a major factor triggering the reactivation mechanism (Van Asch et al. 2009; Xu and Zhang 2010; Fowze et al. 2012; Marco et al. 2018). Some scholars (Tacher et al. 2004; Tommasi et al. 2013; Vassallo et al. 2015; Liu and Li 2015; Conte and Troncone 2018; Tu et al. 2019) focused on the influence of rainfall increasing pore water pressure on landslides. However, ancient landslides vary owing to the complexity in material composition and event history. Published case histories of the reactivation of ancient landslides and long-term monitoring measurements are necessary to depict reliable scenario results and trigger factors and to characterize landslide mechanisms, which provide an in depth analysis of the reactivation mechanism of ancient landslides. To meet this need, Massey et al. (2013) detailed the importance of understanding the behavior of reactivated landslides. Detailed knowledge of the processes is surprisingly scant owing to the lack of datasets. However, the development of the sliding surface has been widely discussed, some scholars (Ferrari et al. 2009; Locat et al. 2014; Huang et al. 2017) proposed a rotational–translational mechanism of a slope with a weak layer, while Xue et al. (2014) proposed a grading creeping–sliding mechanism for a reactivated ancient landslide. Few studies have focused on heavy rainfall-induced landslides with multiple soft layers distributed vertically.

In this study, we study the reactivation mechanism of the Chengnan landslide and provide a comprehensive analysis of the site investigation data, surface displacement monitoring data, deep displacement monitoring data, finite element analysis, and limit equilibrium analysis. The results of the analyses revealed the rainfall-induced reactivation mechanism of the Chengnan landslide with multiple soft layers. Based on this case study, from a scientific and technical point of view, we propose mitigation measures to prevent this similar kind of landslides.

## Study area

The study area is located in Meigu County, Xichang City, Sichuan Province, China. Figure 1 shows the area of a giant ancient landslide that stretches from Meigu County to Daguoire (referred to as the Meigu ancient landslide). This ancient landslide has a width of 2000–3500 m, a length of 1000–1500 m, a thickness of 150–200 m, and a volume of 60 million $m^3$. The bedrock of this landslide is sandstone, fine sandstone, and mudstone in the Dongchuan formation. According to the geological survey from the Xichang Geological Survey Department, the Meigu ancient landslide is a stable ancient landslide.

This stable situation was disturbed by a county extension project in 2002. The road located along the frontal part of the Meigu ancient landslide from Xichang to Meigu used to be the only road from the neighboring regions into Meigu County. After the extension project, another county road was constructed. During the construction, tons of excavated soils were relocated on the top of ancient landslide, deforming the slope and affecting road surface settlements, which indicated the partially reactivation of Meigu ancient landslide. The partially reactivated ancient landslide is referred to as the Chengnan landslide, which can be seen in Fig. 1.

## Description of the Chengnan landslide

The Chengnan landslide is located at the southwest entrance of Meigu County, along the left bank of Lamosede gully. The Xichang–Meigu road passes through the frontal part of Chengnan landslide, and county road surrounds the entire Chengnan landslide.

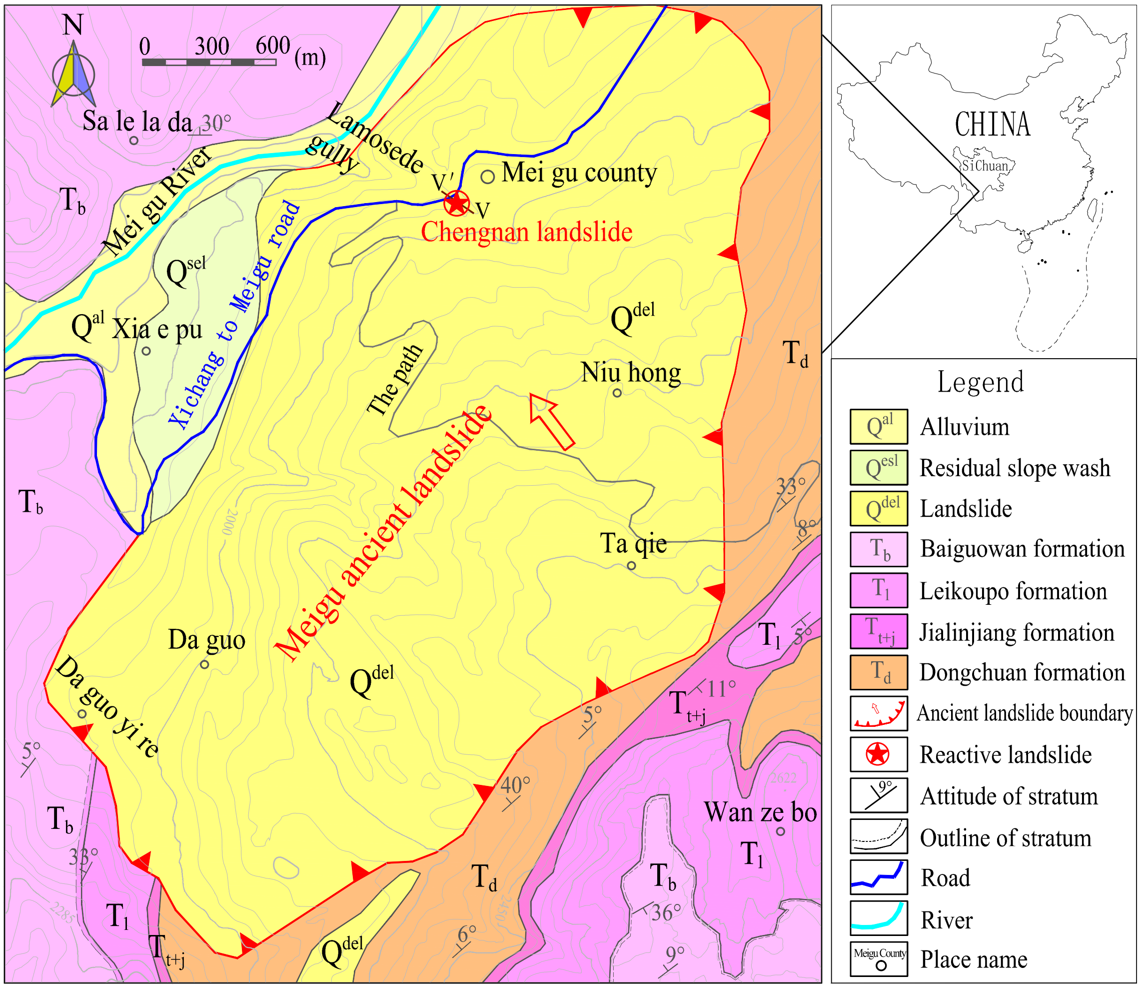


**Fig. 1** Study area

This landslide is tongue shaped. After the reactivation of the Chengnan landslide, a reshaping project was undertaken to reduce the loading on the upper part of the landslide area located above the Xichang–Meigu road in 2006. Afterward, the reshaped Chengnan landslide appeared stair-like, with a slope angle of 21°, whereas the slope angle of the lower part beneath the Xichang–Meigu road was 35°. The Chengnan landslide is 220 m in length and 180 m in width; the difference in altitude between the frontal part and the trailing edge is 130 m; its volume is 500,000 $m^3$ and the main sliding direction is at 330°. A panoramic view of the Chengnan landslide is shown in Fig. 2.

Since the reactivation of the Chengnan landslide began in 2002, deformation has become more and more serious as a result of rainfall. Several signs of deformation were found along the Xichang–Meigu road area, including ring cracks on the trailing edge expanding to 100 m, vertical displacement reaching 20 cm, and retaining walls bulging by 30 cm (Fig. 3a). The buildings located at the entrance of Meigu County experienced deformation owing to the movement of Chengnan landslide (Fig. 3b). Fig. 3c shows the settlement of county road, with cracks measuring 20–30 cm. Tension cracks (with a width of 3–5 cm) were found on the retaining wall along the Xichang–Meigu road (Fig. 3d).

In order to obtain the characteristics of Chengnan landslide as well as the development of its deformation, several site investigations and monitoring projects were carried out. The Chengnan landslide topographic surveys were conducted. Two exploration profiles (V-V′ and VI-VI′) were set for the investigation, including four exploration pits (labeled TC01, TC02, TC03, and TC04), six drilling boreholes (labeled BK01, ZK11, BK02, ZK12, ZK13, and ZK14), and one exploration adit. Monitoring projects were set along V-V′ profile, including six surface displacement monitoring points (labeled P2, P48, P4, P45, P35, and P18), and two deep borehole displacement monitoring points (labeled BK01 and BK02). Various surveys and measurement points were shown in Fig. 2.

The depth of the sliding surface was determined to be 14 m according to the 2005 site investigation results; no signs of deeper sliding were evident at that time. Therefore, treatment projects were initiated to stabilize the sliding mass above the sliding surface at a depth of 14 m. Treatment projects were undertaken since 2006, including measures to reduce loads, improve the drainage system, and to install anti-sliding piles (Fig. 4). After the load-reduction project, the slope body above the Xichang–Meigu road was shaped like a staircase with six steps. The drainage system included

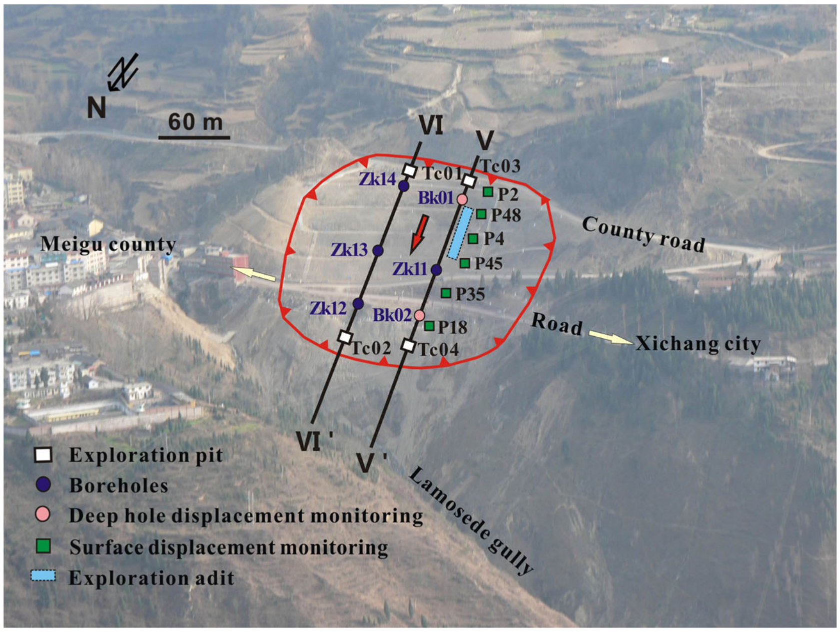


**Fig. 2** Photograph of the Chengnan landslide (2006)

drainage channels on the ground surface and adit. A total of 32 anti-sliding piles were constructed beneath the Xichang–Meigu road; the pile spacing was 5 m, sectional dimension was $2 \times 3$ m$^2$, and their lengths were 18–22 m. In August 2006, the landslide treatment projects were completed. Surface displacement monitoring data from August 2006 to July 2007 demonstrated that the treatment measures had a positive effect.

## Study methods and results

### Site investigation and geotechnical survey

Two exploration drilling profiles were set for the investigation, including six drilling boreholes, four exploration pits, and one exploration adit with a length of 63 m, a width of 1.2 m, and a height of 1.8 m (Figs. 2 and 5). Based on the site exploration results,

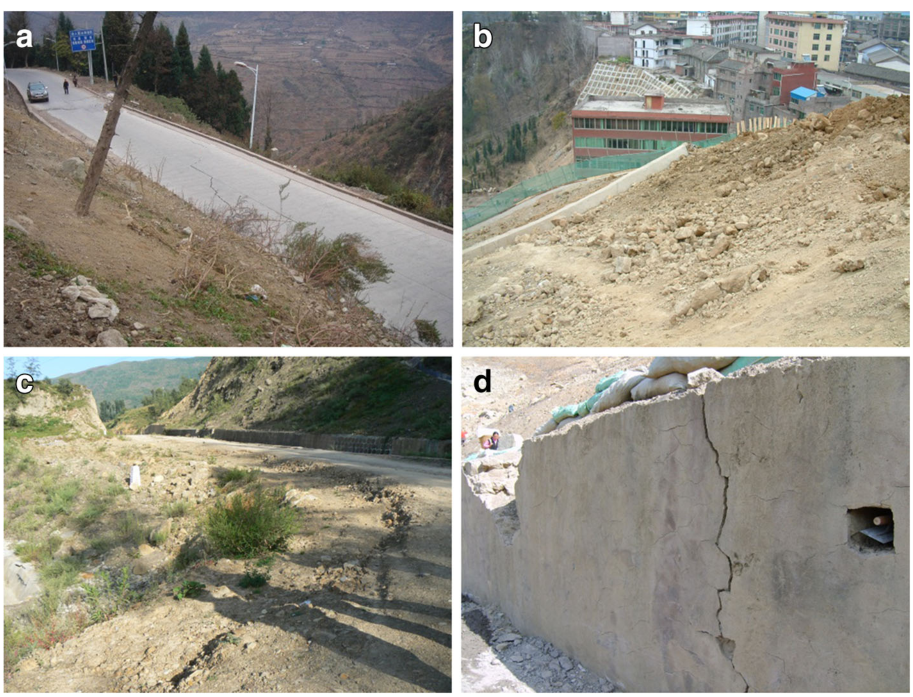


**Fig. 3** Photographs of deformation caused by the Chengnan landslide. (a) Cracks on the Xichang–Meigu road. (b) Deformed slope becoming a threat to adjacent buildings. (c) Settlement along the beltway crossing the trailing edge of the Chengnan landslide. (d) Cracks on the retaining wall along the Xichang–Meigu road


**Fig. 4** Treatment projects. (a) Stair shape after reducing load. (b) Drainage channel on the slope surface. (c) Adit inside of the slope body. (d) Construction of anti-sliding piles

which were recorded from boreholes BK01 and BK02, the deepest borehole in the V–V′ profile had a depth of 56.5 m.

### Composition materials

The main composition materials include cobbles and boulders, silt with multiple soft layers, human-activity deposits, and residual diluvium. These materials were complexly distributed inside the landslide body, as shown in Fig. 5. Special attention should be paid to the findings from BK02 borehole. Among the gravel soil layers, four soft layers were recorded. The first soft layer was at a depth of 14 m and had a thickness of 0.6 m. The second soft layer was at a depth of 28 m and had a thickness of 0.6–0.8 m. The third soft layer was at a depth of 40.5 m and had a thickness of 4 m. The fourth soft layer was at a depth of 55 m and had a thickness of 0.6–1 m. Partial borehole samples from BK02 borehole are shown in Fig. 6. The soft layers are indicated by a yellow arrow.

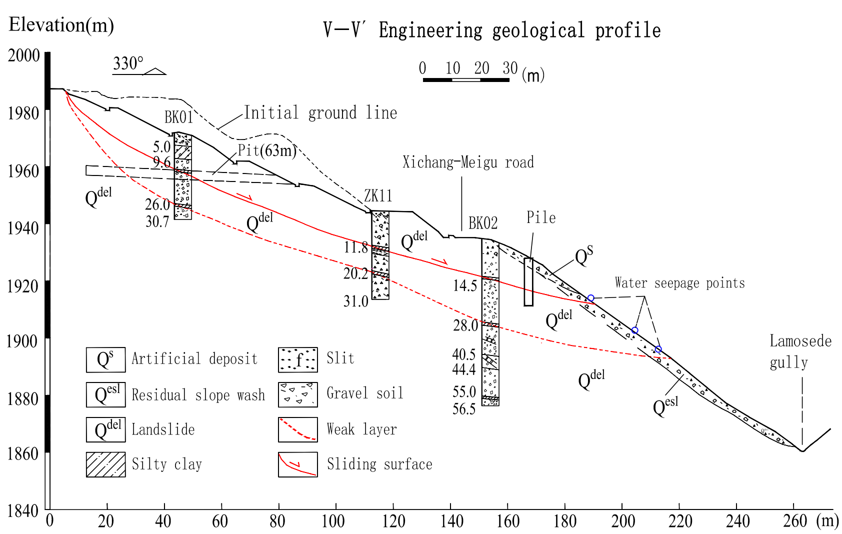


**Fig. 5** V–V′ engineering geological profile


**Fig. 6** (a) BK02 borehole sample, where the first soft layer was found at 14 m. (b) BK02 borehole sample, where the second soft layer was found at 28 m

Sliding surface

BK01 borehole was located on the trailing edge of the Chengnan landslide. A clay layer with a thickness of 0.5 cm was found at a depth of 9.6 m, and striations were found on the borehole clay sample. Meanwhile, inside the adit, a clay zone was found at a depth of 36 m, and dislocation of the clay was observed. Fig. 7a shows that the scrip was broken because of the tension from the sliding zone, which occurred during the rainy season. Compared with samples from BK01 borehole, a clay layer was also found inside of the adit, which appeared to be the same clay layer as that inside of the sliding body.

Scratches on the clay layer at a depth of 14 m are shown in Fig. 7b. A borehole sample from BK02 shows that the clay was yellow and gray in color and was in a plastic state. The dip/dip direction of the striated surface was 15°/330°, basically coincident with the dip/dip direction of the Chengnan landslide sliding surface. Both borehole data and observations from the adit revealed that several soft layers exist inside the sliding body of the Chengnan landslide. Although several soft layers were found, most of these were stable, except for one, the first sliding surface of the Chengnan landslide, which was at a depth of 14 m under the ground surface. Treatment projects were undertaken from 2005 to 2006 to inhibit the further slide of the Chengnan landslide along this sliding surface.

Groundwater

There was no stable groundwater level in the boreholes during the dry season according to the 2005 site investigation, and the groundwater inside the exploration adit was very limited. During the rainy season, groundwater overflowed at several locations at the Chengnan landslide toe. After the rainy season, during the construction of the anti-sliding piles, groundwater was stored at the bottom of the anti-sliding pile hole located at the landslide toe (Fig. 8a). Water seepage points were found along the adit during the rainy season, and Fig. 8b shows a stream of groundwater flowing out from the adit wall. These indicated that the adit worked as a drainage channel for groundwater. However, after the treatment projects were completed, some deformation still existed, with cracks appearing on the adit and drainage channels, rainwater penetrating the deeper landslide body, and the stream of groundwater in the adit reducing.

Deformation of the landslide mass continued to become more serious, eventually breaking the adit. The breakage occurred at the first sliding surface. Therefore, the groundwater inside the adit permeated the first sliding surface and penetrated into the deeper part of the landslide body. Later, this issue contributed to the formation of a deeper sliding surface in the Chengnan landslide.

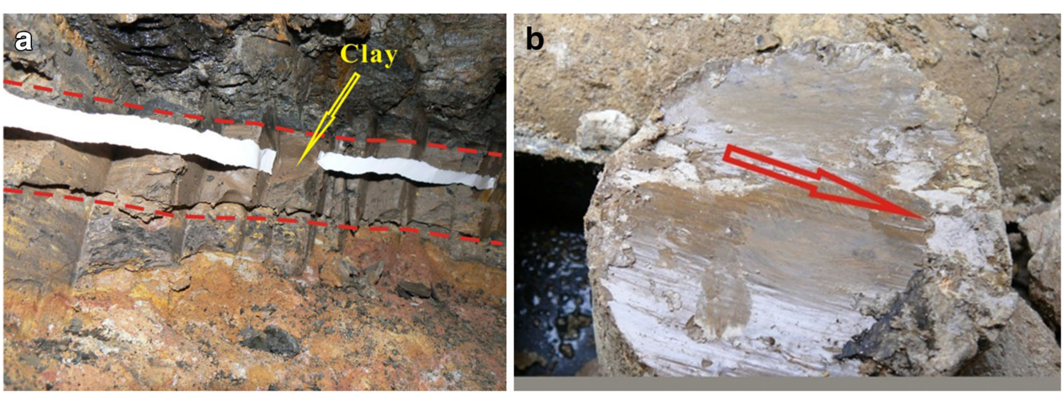


**Fig. 7** (a) Broken scrip at the soft layer at a depth of 36 m of the adit. (b) Borehole sample from BK02 at a depth of 14 m, showing striation on clay

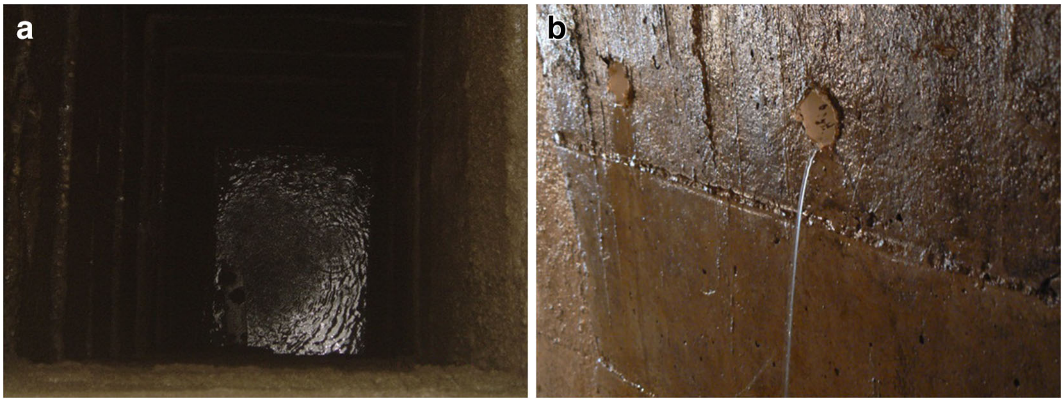


**Fig. 8** (a) Water stored at the bottom of the anti-sliding pile hole. (b) Groundwater flowing out from the adit wall

## In situ monitoring

After the treatment projects were undertaken, a 3-year monitoring program (2006–2008) was implemented to measure deep and surface displacements.

### Surface displacement monitoring

The treatment projects were completed in August 2006, after which a ground surface displacement monitoring project was undertaken. Six sample points (labeled P2, P48, P4, P45, P35, and P18) were distributed along the V–V′ profile from the trailing edge to the frontal part of the landslide, as shown in Fig. 2. P18 was set on the top of one anti-sliding pile. The surface displacement monitoring started from August 2006; and this work lasted for three rainy seasons. The displacement data combined with precipitation data are shown in Fig. 9.

The first raining season after the treatment projects were completed ran from August, 2006 and May, 2007. According to the surface displacement monitoring data (Fig. 9), the P4 point which was located in the head area of Chengnan landslide showed the cumulative displacement was 120 mm, while the P18 point which was located above the anti-sliding pile at the Chengnan landslide toe showed the cumulative displacement was 65 mm. After such interval, the displacement increment tended to be zero, which showed the treatment projects had stabilized the sliding mass above the sliding surface at a depth of 14 m.

During the second rainy season, from June 2007 to June 2008, the study area experienced extremely heavy rainfall, often lasting for several days. The highest amount of precipitation recorded in July was 240 mm. The values exceeded all average precipitation records in Meigu County. Consequently, the increment of surface deformation of P4 was 730 mm, with the cumulative displacement up to 850 mm, while the increment of surface deformation of P18 was 240 mm, with the cumulative displacement up to 300 mm. These monitoring data showed that the Chengnan landslide was reactivated again.

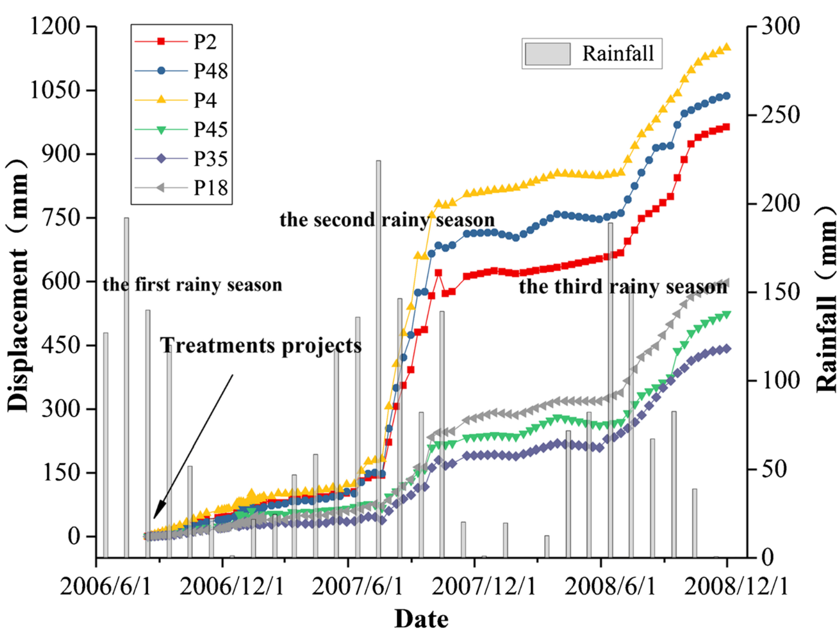


**Fig. 9** Combined graphs of surface displacement data and precipitation record

The third rainy season ran from June 2008. The displacement increment at P4 is 300 mm, the cumulative displacement was up to 1150 mm. The displacement at P18 showed a clear increase, with cumulative displacement up to 600 mm.

In conclusion, from the surface displacement data, it can be seen that heavy rainfall had a significant influence on the deformation of Chengnan landslide. The displacement of Chengnan landslide increased sharply just after each rainy season. The deformation at the trailing edge of the landslide was greater than that at the frontal part.

### Deep displacement monitoring

To determine the reason for the continuous deformation of the landslide, it was necessary to undertake a deep displacement monitoring project after the second rainy season. The deep displacement monitoring project was conducted from June 4, 2007 to June 27, 2008. Two deep monitoring holes were set along the monitoring profile: BK01 borehole was located at the trailing edge of the landslide, at a depth of 30 m, and BK02 borehole was located at the frontal part of the landslide, at a depth of 53.5 m; these locations are shown in Figs. 2 and 5.

The cumulative displacement data for BK01 are shown in Fig. 10. Monitoring began on June 22, 2007, with displacement at 4 mm. However, during the rainy season, data obtained on July 19, August 24, and September 9 indicated that the cumulative displacement had increased to 200 mm. The gradually increasing trend became more subtle after the rainy season. By June 27, 2008, the cumulative displacement for BK01 reached 330 mm. By analyzing the curve of cumulative displacement, one can identify an obvious turning point at a depth of 9.6 m; this position was also found to be that of the first sliding surface. The cumulative horizontal displacement at this depth was 300 mm. This displacement was very close to the surface displacement of the monitoring hole, indicating that the first sliding surface was active during the monitoring period. At the end of the monitoring project, a probe rod could not reach the bottom of the monitoring hole; it got stuck at a depth of 9.6 m. As a result, no further data were obtained after this event.

The cumulative displacement data for BK02 are shown in Fig. 11. At the onset of monitoring, June 22, 2007, the displacement was very small at 3 mm. Before September 2007, the cumulative displacement at the surface of BK02 was 10 mm, the cumulative displacement of BK01 was also small at the same period, indicating clearly that the anti-sliding piles constructed at the frontal part of the landslide were effective. However, the horizontal displacement increased sharply, with the cumulative displacement reaching 205 mm from September 2007 to June 2008. By analyzing the curve of cumulative displacement in Fig. 11, one can identify an active sliding surface at a depth of 14 m at the beginning of rainy season. After the rainy season (November 2007), the second sliding surface became active at a depth of 28 m. The horizontal displacement of the first sliding surface was 120 mm, and the horizontal displacement of the second sliding surface was 55 mm. The dominant sliding surface was the first sliding surface, which was found at a depth of 14 m. During the

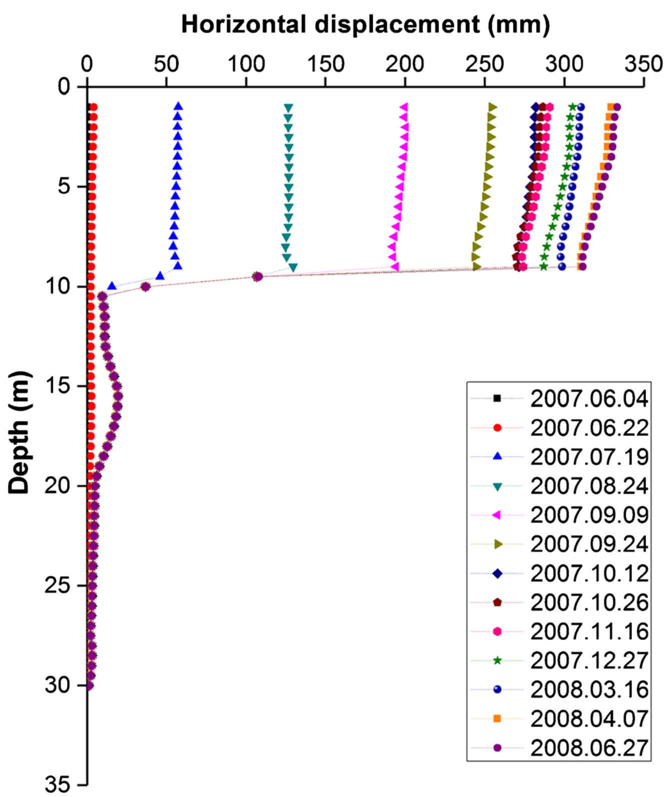


**Fig. 10** Cumulative displacement of BK01

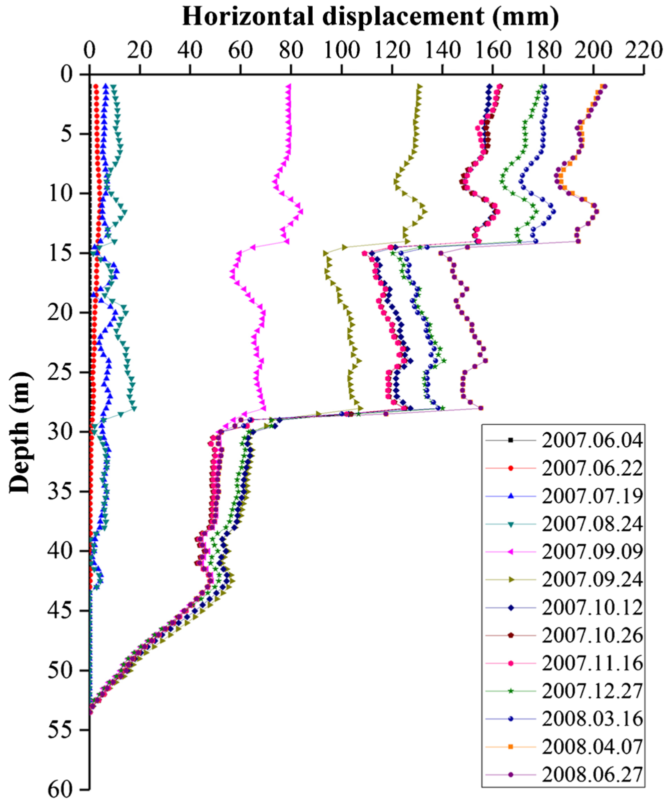


**Fig. 11** Cumulative displacement of BK02

monitoring interval between November 16, 2007, and June 27, 2008, these two sliding surfaces became active simultaneously, with horizontal displacements of 30 and 31 mm, respectively. The same event occurred at BK02, but the probe rod could not reach the bottom of the monitoring hole because of the large deformation at a depth of 28 m.

### Finite element analysis

Finite element analysis was performed to examine the failure mechanism, and preliminary stress–strain analyses were conducted using MIDAS/GTS to calculate the safety factor using the shear strength reduction method (Griffiths and Lane 1999; Xu and Zhang 2010; Paola et al. 2012).

In the shear strength reduction method, one applies a strength reduction coefficient $F'$ to obtain new values of $C_F$ and $\psi_F$ and calculate the slope stability by using the following formulas (Tsai et al. 2008; Xue et al. 2018):

$$C_F = C/F'. \quad (1)$$

$$\psi_F = \arctan\left(\tan\psi/F'\right). \quad (2)$$

To obtain the safety factor, the strength reduction factor ($F'$) needs to be gradually increased until the reduced strength parameters ($C_F$ and $\psi_F$) bring the slope into a failure state (numerical no convergence occurs within a specified maximum number of iterations). At that time, the safety factor for the landslide is equal to the strength reduction factor, i.e., $Fs = F'$ (Wang et al. 2014).

Based on the site investigation and exploration results (Fig. 2), the engineering geological profile V–V′ (Fig. 5) was used to analyze the stability of Chengnan landslide. Finite element model was built based on the site characteristics of Chengnan landslide as well as the morphological character of this landslide before Chengnan landslide was reactivated. The components of the simulated model included excavated mass, three gravel soil layers, and two clay layers (Fig. 12).

The model was 313 m in length, with a height of 164 m on the left bound and a height of 32 m on the right bound. The model consisted of 5643 grids. Based on the monitoring results of BK02 (Fig. 9), the gravel soil 3 from the model was stable. The left and right boundaries of the finite element model were set as no-horizontal-displacement boundaries, and the bottom boundary was set as a no-horizontal and no-vertical-displacement boundary, the slope surface of this model was free. The initial stress condition was self-weight (Fig. 12).

The geotechnical parameters were determined from laboratory tests, literature values, and empirical engineering experience (Shen et al. 2006; Song et al. 2012). The values of these parameters are listed in Table 1. Data which are shown in parentheses are saturated shear strength of clay layers by laboratory tests.

Several researchers (Locat et al. 2014; Valore et al. 2017; Ziccarelli et al. 2017) have demonstrated the softening effect of water to reduce the mechanical strength of clay layer. In this

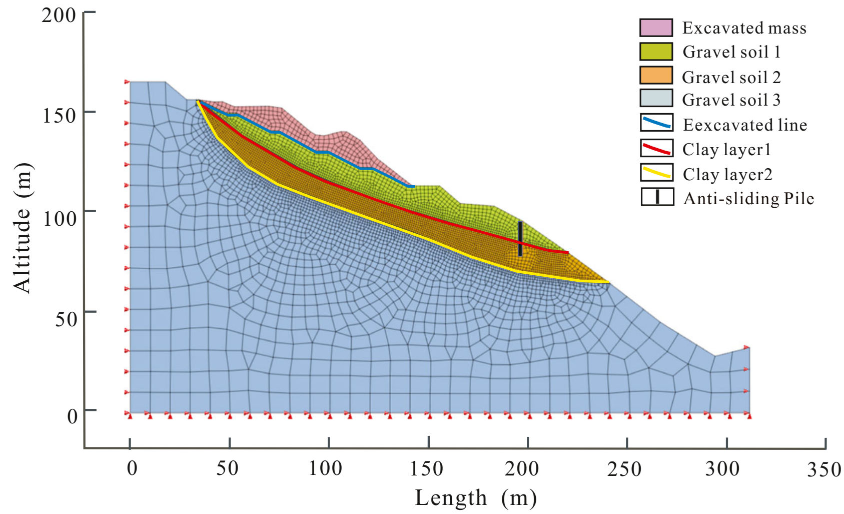


**Fig. 12** Finite element analysis model of the Chengnan landslide

paper, the softening effect of water to reduce the mechanical strength of clay layer was firstly considered; then, the safety factors were calculated at different stages by using the finite element strength reduction method. The Mohr–Coulomb failure criterion was adopted for the analyses. According to the Mohr–Coulomb model, when the shear stress reaches a certain value, the material yields. Furthermore, this model can be used to determine the most potentially critical sliding surface. The numerical simulation of Chengnan landslide can be divided into three stages.

The first stage: In order to simulate the first reactivation of Chengnan landslide, the reduction of the shear strength of the clay layer 1 with a depth of 14 m was considered.

The second stage: After the first reactivation of Chengnan landslide, treatment projects (including reduce loads, anti-sliding piles and the drainage system) were undertaken. Groundwater was drained out of the slope by the drainage system (Fig. 8b), therefore, the softening effect which the water played on the clay layers was not considered in this stage. The reduce loads and anti-sliding piles were simulated in the model.

The third stage: During the second rainy season, groundwater infiltrated into the deeper landslide body, the reduction of the shear strength of clay layer 1 as well as clay layer 2 was considered in this stage. The second reactivation of Chengnan landslide was simulated.

The stress–strain distribution results at every stage and the safety factor (*Fs*) were calculated, as shown in Fig. 13. **The first stage:** Chengnan landslide slid along the first clay layer (i.e., the first sliding surface) at a depth of 14 m, and the safety factor was 0.97 (Fig. 13a). **The second stage:** after the treatment projects were undertaken, a safety factor of 1.21 was calculated for the first sliding surface (Fig. 13b). **The third stage:** After heavy rainfall, groundwater infiltrated into the deeper landslide body and softened the second clay layer, which was located at a depth of 28 m, lowering the shear strength of the second softened layer. Consequently, a new sliding surface was well developed, and the corresponding safety factor of the Chengnan landslide along this sliding surface was 1.02. Because the second sliding surface was deeper than the anti-sliding piles, the anti-sliding piles had no beneficial effect on the stability of landslide along this sliding surface, as shown in Fig. 13c.

The results obtained from the FEM analysis on the second and third stages are in good agreement with the deep displacement monitoring dates of BK02 borehole (Fig. 14). It also indicates the results of FEM simulation are reasonable.

**Table 1** Geotechnical parameters used in the stress–strain analysis

| | Excavated mass | Gravel soil 1 | Gravel soil 2 | Gravel soil 3 | Clay layer 1 | Clay layer 2 | Barrette pile |
|---|---|---|---|---|---|---|---|
| Dry specific weight (kN/m$^3$) | 20 | 20 | 20 | 20 | 18 | 18 | 26 |
| Saturated specific weight (kN/m$^3$) | 21 | 21 | 21 | 21 | 18.5 | 18.5 | |
| Cohesion (kPa) | 5 | 5 | 5 | 5 | 42(21) | 40(20) | |
| Friction angle (°) | 25 | 25 | 28 | 28 | 20(15) | 20(17) | |
| Young's modulus (kPa) | 200,000 | 200,000 | 800,000 | 800,000 | 50,000 | 150,000 | 30,000,000 |
| Poisson's modulus | 0.3 | 0.3 | 0.3 | 0.3 | 0.32 | 0.32 | 0.17 |

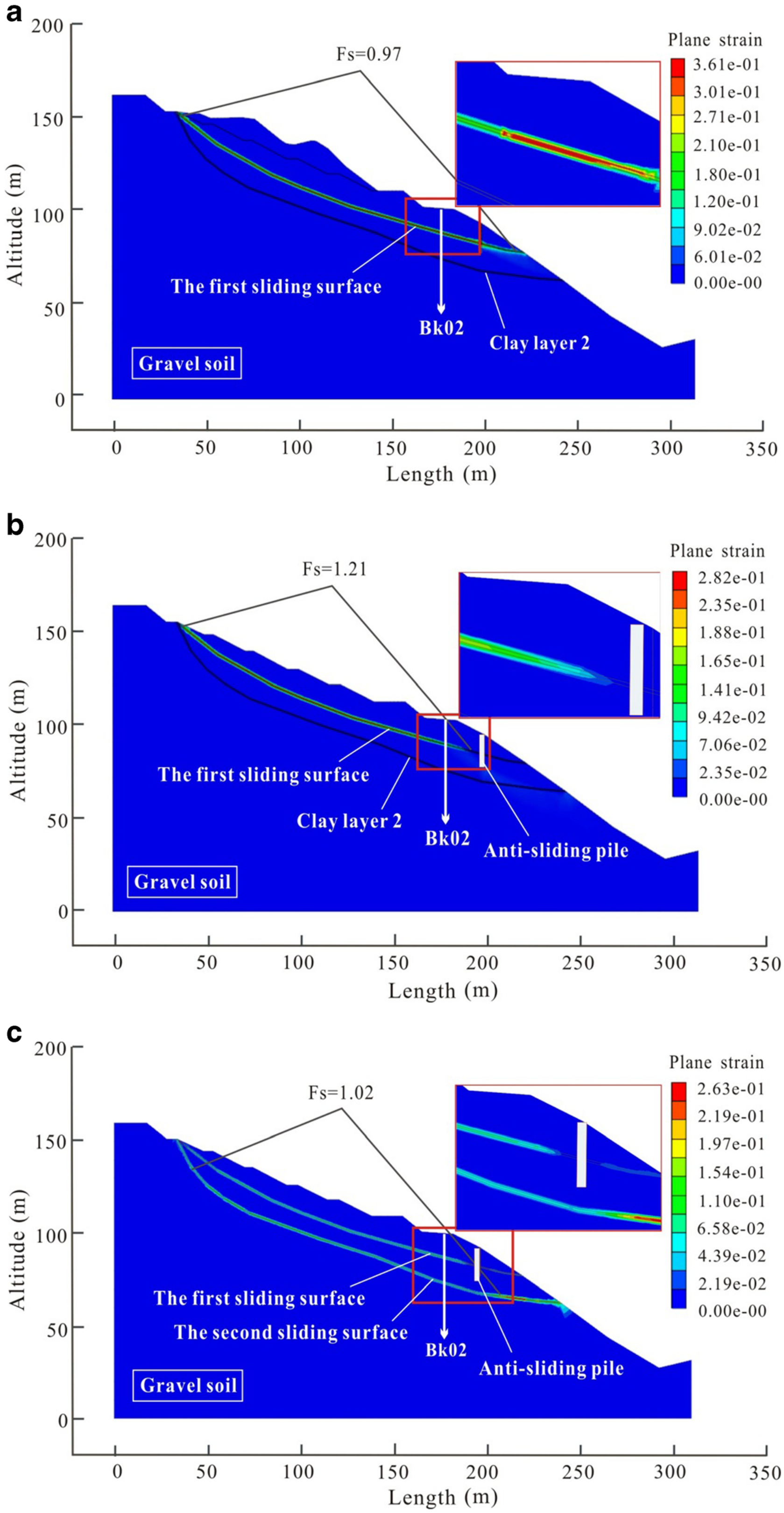


**Fig. 13** Finite element calculation results of the Chengnan landslide. (a) The first stage, the Chengnan landslide slid along the first sliding surface at a depth of 14 m. (b) The second stage, after treatment projects were undertaken, the Chengnan landslide became stable. (c) The third stage, the Chengnan landslide slid along the second sliding surface at a depth of 28 m; the anti-sliding piles failed

### Limit equilibrium stability analysis

Based on the inclinometer measurement results, the sliding surfaces where the upper two inclinometers BK01 and BK02 were located were detected to occur at depths of 14 and 28 m below the ground surface, respectively, coinciding with the depth of the first and second clay layers. As demonstrated by the FEM analysis, two sliding surfaces developed along the two clay layers; their positions are very consistent with the inclinometer measurement results.

The limit equilibrium method is the main method used to analyze the stability of soil slope (Janbu 1954; Morgenstern and Price 1965; Sarma 1973). Morgenstern-Price slice method was applied to analyze the stability of the Chengnan landslide. The factor of safety was 0.99 when the Chengnan landslide first reactivated along the first sliding surface with a depth of 14 m. After the treatment projects were completed, the factor of safety was 1.25. The factor of safety was 1.03 when the Chengnan landslide reactivated again along the second sliding surface with a depth of 28 m. The results of the limit equilibrium stability analysis and the results of the FEM strength reduction calculation are similar to each other while a slightly larger on the results of the limit equilibrium stability analysis.

## Reactivation mechanism and lessons

### Reactivation mechanism of the Chengnan landslide

The following conclusions can be drawn from the results obtained from the site investigation, the in situ monitoring and finite element analysis, the main influencing factors of landslide reactivation, and the reactivation mechanism of the Chengnan landslide:

It is clear from the site investigation materials that the main deposit of this ancient landslide consists of gravel soils, with several soft layers inside. These clay layers were distributed at depths of 14, 28, 40.5, and 55 m, as shown in Fig. 5. Gravelly soil is permeable, so rainwater penetrates into the landslide body, and the pore pressure of groundwater can compromise slope stability (Liu and Li 2015; Christofer et al. 2017). The soft clay layer underneath the gravel soil is impermeable, and groundwater softens this layer and reduces soil strength (Locat et al. 2014; Valore et al. 2017; Ziccarelli et al. 2017), leading to the layer becoming a sliding surface. In conclusion, the soil distribution of Chengnan landslide facilitated the formation of several sliding surfaces during the reactivation of the landslide once the groundwater affected its stability.

Rainfall is considered as the main factor that triggered the reactivation of the Chengnan landslide. Based on the displacement data analysis, slope deformation mainly depended on the effect of rainfall. Observations made outside the rainy season reveal no groundwater table, a dry adit, and a lack of groundwater at the landslide toe. However, during the rainy season, several groundwater overflow points were found at the toe area. After the construction of anti-sliding piles, groundwater was collected in the foundation of the anti-sliding piles; groundwater was also found inside the adit (Fig. 8). Additionally, ground displacement monitoring data (Fig. 9) showed corresponding

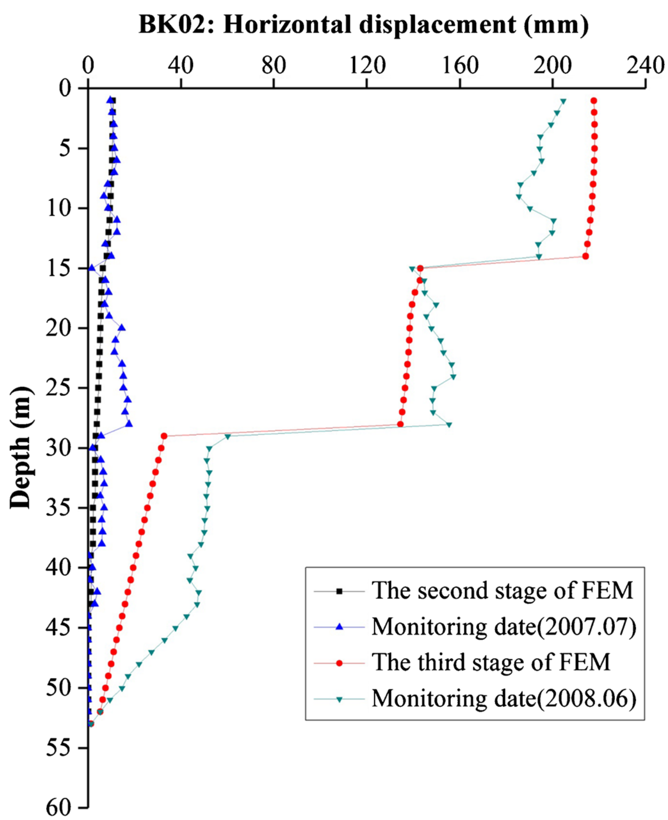


**Fig. 14** Comparison between the FEM simulated data and the site measured displacement data from deep borehole-BK02

results. Outside the rainy season (September 2006 to May 2007 and September 2007 to May 2008), displacement of the Chengnan landslide was relatively small, with accumulation displacement being 80 mm at a velocity of <0.35 mm/day; however, during the rainy seasons (June 2007 to September 2007 and June 2008 to September 2008), the landslide displacement increment was 650 mm, with a velocity of >6 mm/day. Deep borehole data from BK01 showed that, before the rainy season (in July 2007), the increment in displacement was 10 mm (Fig. 11), but, after the rainy season (between September 2007 and June 2008), the displacement increment was 205 mm; these differences in displacement can be considered as proof of the influence of rainfall on landslide stability. Therefore, the rainfall is the major factor influencing the deformation of Chengnan landslide, and the deformation rate has a positive correlation with the rainfalls.

By comprehensive analysis of the above influencing factors, the reactivation of Chengnan landslide can be concluded as follows:

(1) The Chengnan landslide was initially reactivated in 2002, sliding along the first soft layer (i.e., the first sliding surface) at a depth of 14 m; at this stage, the safety factor was 0.97 (Fig. 13a). After the formation of the first sliding surface at a depth of 14 m, treatment measures were undertaken in 2006, which included reducing loads, improving drainage channel, and installing barrette piles (Figs. 4 and 5); these measures yielded a positive result, stabilizing the Chengnan landslide, and at this stage, the safety factor was 1.21 (Fig. 13b).

(2) Since 2007, more and more cracks were developed in the upper part and the ground surface of landslide, and the adit and other drainage channels were also damaged. Through these cracks, the heavy rainfalls significantly enhance the rainwater infiltration into the interior of landslide body. On the one hand, it makes for saturation and triggers a high pore water pressure in slip mass, finally increasing the downslide strength of slide (Xia et al. 2013; Liu and Li 2015; Christofer et al. 2017; Tu et al. 2019); on the other hand, the softening effects of water reduce the mechanical strength of the second clay layer (Locat et al. 2014; Valore et al. 2017; Ziccarelli et al. 2017). Consequently, a new sliding surface (i.e., the second sliding surface) at a depth of 28 m was developed (Figs. 11 and 13c), the Chengnan landslide was reactivated again in 2007 along the second sliding surface. Because the second sliding surface was deeper than the anti-sliding piles, the anti-sliding piles failed. At this stage, the safety factor of Chengnan landslide was 1.02 (Fig. 13c).

Based on the analysis results and referring to the recent classification of landslide types (Hungr et al. 2014), a multilayer creeping–tension mechanism controlled by multiple soft layers of the Chengnan landslide was proposed.

## Lessons

This study can help focus our attention to similar kinds of landslide with complex composition materials. Such complexity causes difficulties in the site investigation; furthermore, it makes it difficult to identify the potential sliding surface. This investigation required increasing the depth of the dominated boreholes. Two or more soft layers contributed to the complex slope behavior during the treatment process.

Among treatment measures, anti-sliding pile is the most common. However, for this kind of landslide with several soft layers, special attention needs to be paid to the anti-sliding pile length during the design (Song et al. 2012). Otherwise, the treatment will fail because of poor understanding of the deeper potential sliding surface.

According to the site investigations and exploration, the Chengnan landslide has several clay soft layers, and the shear strength of clay decreased under the wetting cycles (Locat et al. 2014; Valore et al. 2017; Ziccarelli et al. 2017), which induced the instability of landslide. Therefore, in order to weaken the influence of the water, it is better to construct more ground drainage channels as well as the ground water drainage channels.

Two sliding surfaces were distributed vertically in the Chengnan landslide. So far, no treatment project is carried out on the second sliding surface. Therefore, a better comprehensive monitoring system should be established. More specific suggestions are proposed: six surface displacement monitoring points and two deep boreholes displacement monitoring points will be set along VI-VI′ profile. Some displacement monitoring points will need to be installed at the Chengnan landslide toe where above anti-sliding piles. The long-term groundwater level monitoring should be conducted inside boreholes BK01, ZK11, and BK02.

## Conclusions

A comprehensive study on the causes of the activation of Chengnan landslide, including site investigation, displacement monitoring, finite element analysis, and limit equilibrium analysis, has been presented. The conclusions derived are as follows:

(1) The Chengnan landslide is a partially reactivated ancient landslide, the sliding body of which contains several soft layers. These soft layers may facilitate the formation of a sliding surface under heavy rainfall conditions.

(2) Deep displacement monitoring data analysis shows a strong direct correlation between precipitation and cumulative displacement of the landslide. Furthermore, the first and second sliding surfaces of Chengnan landslide were observed.

(3) The Chengnan landslide underwent two reactivations, which occurred along the first and second soft layers. The depths of the two soft layers were 14 and 28 m. The reactivation mechanism is considered to be a multilayer creeping–tension mechanism controlled by multiple soft layers.

(4) Efficiently mitigating this kind of landslide requires some considerations: A detailed site reconnaissance of soft layers and groundwater should be performed. More laboratory tests are required to gain a complete understanding of the soft layer materials, and a more accurate slope stability analysis should be conducted. In order to reduce the adverse influence of water on soft layers, it is necessary to construct more ground drainage channels as well as the ground water drainage channels.

## Acknowledgements

The authors of this paper gratefully acknowledge the financial assistance provided by the State Key Laboratory of Geohazard

Prevention and Geoenvironment Protection Independent Research Project (SKLGP2016Z021) and the Key Program of the State Key Laboratory of Geohazard Prevention and Geoenvironment Protection (SKLGP2011Z002).

## References

Anbarasu K, Sengupta A, Gupta S, Sharma SP (2010) Mechanism of activation of the Lanta Khola landslide in Sikkim Himalayas. Landslides 7:135–147
Christofer K, Harianto R, Alfrendo S (2017) Effect of variations in rainfall intensity on slope stability in Singapore. Int Soil Water Conserv Res 5:258–264
Conte E, Troncone A (2018) A performance-based method for the design of drainage trenches used to stabilize slopes. Eng Geol 239:158–166
Ferrari A, Laloui L, Bonnard C (2009) Hydro-mechanical modelling of a natural slope affected by a multiple slip surface failure mechanism. Comput Model Eng Sci 52(3):217–235
Ferrari A, Ledesma A, González D, Corominas J (2011) Effects of the foot evolution on the behaviour of slow-moving landslides. Eng Geol 117:217–228
Fowze JSM, Bergado DT, Soralump S, Voottipreux P, Dechasakulsom M (2012) Rain-triggered landslide hazards and treatment measures in Thailand: from research to practice. Geotext Geomembr 30:50–64
Griffiths DV, Lane PA (1999) Slope stability analysis by finite elements. Géotechnique 49(3):387–403
Huang MS, Fan XP, Wang HR (2017) Three-dimensional upper bound stability analysis of slopes with weak interlayer based on rotational-translational mechanisms. Eng Geol 223:82–91
Hungr O, Leroueil S, Picarelli L (2014) The Varnes classification of landslide types, an update. Landslides 11(2):167–194
Janbu N (1954) Application of composite slip surface for stability analysis. In: Proceedings of the European Conference on Stability of Earth Slopes, Stockholm, pp 43–49
Liu QQ, Li JC (2015) Effects of water seepage on the stability of soil-slopes. Science Direct:29–39
Locat J, Leroueil S, Locat A, Lee H (2014) Weak layers: their definition and classification from a geotechnical perspective. Part of the Advances in Natural and Technological Hazards Research book series (NTHR, volume 37): 3–12
Marco R, Maurizio Z, Alessio F, Camillo AF (2018) On the reactivation of a large landslide induced by rainfall in highly fissured clays. Eng Geol 235:20–38
Massey CI, Petley DN, McSaveney MJ (2013) Patterns of movement in reactivated landslides. Eng Geol 159:1–19
Morgenstern NR, Price VE (1965) Analysis of stability of general slip surface. Geotechnique 15:79–93
Paola G, Laura S, Luca A, Marco C (2012) The February 2010 large landslide at Maierato, Vibo Valentia, southern Italy. Landslides 2:255–261
Sarma SK (1973) Stability analysis of embankments and slopes. Geotechnique 23:423–433
Shen Q, Chen CX, Wang R (2006) Analysis of mechanical parameters of slip surface for basalt landslide in Yunnan. Rock Soil Mech 12:2309–2313
Song YS, Hong WP, Woo KS (2012) Behavior and analysis of stabilizing piles installed in a cut slope during heavy rainfall. Eng Geol 129–130:56–67 in Chinese
Tacher L, Bonnard C, Laloui L, Parriaux A (2004) Modelling the behaviour of a large landslide with respect to hydrogeological and geomechanical parameter heterogeneity. Landslides 2:3–14
Tommasi P, Boldini D, Caldarini G, Coli N (2013) Influence of infiltration on the periodic re-activation of slow movements in an overconsolidated clay slope. Can Geotech J 50(1):54–67
Tsai TL, Chen HE, Yang JC (2008) Numerical modeling of rainstorm-induced shallow landslides in saturated and unsaturated soils. Environ Geol 55:1269–1277
Tu GX, Huang D, Deng H (2019) Reactivation of a huge ancient landslide by surface water infiltration. J Mt Sci 16(4):806–820
Valore C, Ziccarelli M, Muscolino SR (2017) The bearing capacity of footings on sand with a weak layer. Geotechnical Research 4(1):12–29
Van Asch WJ, Malet JP, Bogaard TA (2009) The effect of groundwater fluctuations on the velocity pattern of slow-moving landslides. Nat Hazards Earth Syst Sci 9:739–749
Vassallo R, Grimaldi MG, Di Maio C (2015) Pore water pressures induced by historical rain series in a clayey landslide: 3D modeling. Landslides 12(4):731–744
Wang JJ, Liang Y, Zhang HP, Wu Y, Lin X (2014) A loess landslide induced by excavation and rainfall. Landslides 11:141–152
Xia M, Ren GM, Ma XL (2013) Deformation and mechanism of landslide influenced by the effects of reservoir water and rainfall, three gorges, China. Nat Hazards 68:467–482
Xu QJ, Zhang LM (2010) The mechanism of a railway landslide caused by rainfall. Landslides 7:149–156
Xue DM, Li TB, Wei YX, Gao MB (2014) Mechanism of reactivated Badu landslide in the Badu Mountain area, Southwest China. Environ Earth Sci 15:79–93
Xue DM, Li TB, Zhang S, Ma CC, Gao MB, Liu J (2018) Failure mechanism and stabilization of a basalt rock slide with weak layer. Eng Geol 233:213–224
Ziccarelli M, Valore C, Muscolino SR, Fioravante V (2017) Centrifuge tests on strip footings on sand with a weak layer. Geotechnical Research 4(1):47–64

**Y. Ren · T. Li (✉) · J. Tang · D. Xue**
State Key Laboratory of Geohazard Prevention and Geoenvironment Protection,
Chengdu University of Technology,
Chengdu, 610059, Sichuan, China
Email: ltb@cdut.edu.cn

**S. Dong**
Civil Engineering Department,
Sichuan College of Architectural Technology,
Deyang, 618000, Sichuan, China